Available online at www.sciencedirect.com

ScienceDirect

Journal of Molecular Structure 890 (2008) 48–56

Journal of
MOLECULAR
STRUCTURE

www.elsevier.com/locate/molstruc

Chemistry of dimolybdenum complexes containing bridging anions of *N*,*N*′-di(3-methoxyphenyl)formamidine

Ying-Yann Wu [a], Chun-Wei Yeh [a], Zhi-Kai Chan [a], Chia-Her Lin [a],
Chia-Hsi Yang [a], Jhy-Der Chen [a,*], Ju-Chun Wang [b]

[a] *Department of Chemistry, Chung-Yuan Christian University, No. 200, Chung Pei Road, Chung-Li, Taiwan, ROC*
[b] *Department of Chemistry, Soochow University, Taipei, Taiwan, ROC*

Received 9 November 2007; received in revised form 16 January 2008; accepted 16 January 2008
Available online 1 February 2008

Dedicated to the memory of Professor F.A. Cotton, a great mentor and friend.

Abstract

Reaction of $Mo(CO)_6$ with excess *N*,*N*′-di(3-methoxyphenyl)formamidine (HDmAniF) in *o*-dichlorobenzene afforded the yellow complex $Mo_2(DmAniF)_4$, **1**. The structure of **1** reveals that the ligands bridge the two metal centers through the two nitrogen atoms, forming two *s-cis*, *s-trans* and two *s-trans*, *s-trans* conformations. Reaction of **1** with Me_3OBF_4 in CH_3CN gave *cis*-$[Mo_2(DmAniF)_2(CH_3CN)_4][BF_4]_2$, **2**, which crystallized in two different forms. The first form, **2**$\cdot CH_2Cl_2 \cdot CH_3CN$, **2a**, showing one BF_4^- anion coordinating to the axial positions of the Mo–Mo bond [$Mo \cdots F = 2.685(4)$ Å], contains two *cis* $DmAniF^-$ ligands which adopt the same *s-cis*, *s-trans* conformation. The other form, **2**$\cdot 0.5CH_2Cl_2 \cdot 0.5CH_3CN$, **2b**, involves two independent molecules. While one [$Mo–Mo = 2.1432(8)$ Å] of the two molecules shows axial interaction by CH_3CN [$Mo \cdots N = 2.692(8)$ Å] and the two *cis* $DmAniF^-$ ligands adopt the same *s-cis*, *s-trans* conformation, the other one [$Mo-Mo = 2.1317(9)$ Å] shows no axial interaction and the two *cis* $DmAniF^-$ ligands adopt different conformations, which are *s-cis*, *s-trans* and *s-cis*, *s-cis*, respectively. The Mo–Mo distance of **2a**, 2.1281(6) Å, is the shortest among the compounds having $Mo_2(\mu_2\text{-}L)_2(CH_3CN)_4$ core, where L is the anionic, cationic or neutral form of a formamidine ligand. Reaction of **2** with $NaOCH_3$ in CH_3OH produced the tetranuclear complex *cis*-$[Mo_2(DmAniF)_2]_2(\mu\text{-}OCH_3)_4$, **3**. The molecule of **3** bears four bridging CH_3O^- groups that link two quadruply bonded moieties and the ligands adopts the *s-trans*, *s-trans* conformation.

Keywords: Dimolybdenum complex; Formamidine; Conformation; *N*,*N*′-di(3-methoxyphenyl)formamidine

1. Introduction

The coordination chemistry of formamidinate compounds has been investigated extensively during recent years [1–5]. Many efforts have been concentrated in their ability to form bridges between metal atoms. Preparations, structures and spectroscopic properties of tetrakis(μ-diarylformamidinato)dimolybdenum complexes of the type $Mo_2(form)_4$, where form is the generic formamidine, were the subjects of several studies [6]. Crystalline $Mo_2(form)_4$ can be prepared by stoichiometric ligand metathesis between the dimolybdenum tetraacetate $Mo_2(O_2CR)_4$ and the lithiated formamidine. A conformational descriptor for diarylformamidine bearing an *m*-alkoxy substituent has been proposed by Ren and co-authors [5b]. Based on their proposition, three stable conformations exist for diarylformamidine which are defined as (a) *s-cis*, *s-cis*- (*s-cis*-/*s-trans*- are defined between the N–C (methine) bond and the ring C–C bond prioritized by the OR group), (b) *s-cis*, *s-trans*-, and (c) *s-trans*, *s-trans*- [5b].

Although dimolybdenum complexes containing *N*,*N*′-di(4-methoxyphenyl)formamidine (HDpAniF) [4] and *N*,*N*′-di(2-methoxyphenyl)formamidine (HDoAniF) [5g,5h]

---

[*] Corresponding author.
E-mail address: jdchen@cycu.edu.tw (J.-D. Chen).

0022-2860/$ - see front matter © 2008 Published by Elsevier B.V.
doi:10.1016/j.molstruc.2008.01.037

have been subjected to several studies, dimolybdenum complex containing their isomeric ligand *N*,*N*′-di(3-methoxyphenyl)formamidine (HDmAniF) has not been structurally characterized. We report herein several dimolybdenum complexes of the types $Mo_2(DmAniF)_4$ and *cis*-$[Mo_2(DmAniF)_2(CH_3CN)_4][BF_4]_2$, and a tetranuclear complex *cis*-$[Mo_2(DmAniF)_2]_2(\mu\text{-}OCH_3)_4$. The syntheses, structures and ligand conformations of these complexes form the subject of this report.

2. Experimental section

2.1. General procedures

All manipulations were carried out under dry, oxygen-free nitrogen by using Schlenk techniques, unless otherwise noted. Solvents were dried and deoxygenated by refluxing over the appropriate reagents before use. Hexanes, THF and diethyl ether were purified by distillation from sodium/benzophenone, acetonitrile from CaH_2, methanol form Mg/I_2 and dichloromethane from P_2O_5. The visible absorption spectra were recorded on a Hitachi U-2000 spectrophotometer. NMR spectra were measured on a Bruker Avance 300 MHz spectrometer. IR spectra were obtained with the use of a Jasco FT/IR-460 plus spectrometer. Elemental analyses were obtained from a PE 2400 series II CHNS/O analyzer.

2.2. Materials

The complexes $Mo_2(DmAniF)_4$ [2b], $[Mo_2(CH_3CN)_{10}][BF_4]_4$ [7], and the ligand *N*,*N*′-di(3-methoxyphenyl) formamidine (HDmAniF) [5a,8] were prepared according to previously reported procedures. The reagents $Mo(CO)_6$, Me_3OBF_4 and MeONa were purchased from Strem Chemical Co.

2.3. Preparation of $Mo_2(DmAniF)_4$ (**1**)

$Mo(CO)_6$ (1.0 g, 3.79 mmol) and HDmAniF (2.43 g, 9.47 mmol) were placed in a flask containing 10 mL *o*-dichlorobenzene. The mixture was then refluxed for 20 h to yield a brown solution. After the mixture was cooled to room temperature, 80 mL MeOH was then added to give a yellow precipitate. The precipitate was filtered, washed by diethyl ether and then dried under reduced pressure to give the yellow product. Yield: 1.72 g (75%). UV–vis: 443 nm (CH_2Cl_2, $\varepsilon = 2636$ $M^{-1}\,cm^{-1}$). ^1H NMR ($CDCl_3$, ppm): 8.54 (s, 4H, C*H*),6.85 (t, 8H, H^{meta}), 6.44 (d, 8H, H^{para}), 6.03 (d, 8H, H^{ortho}), 5.80 (s, 8H, H^{ortho}), 3.26 (s, 24H, OC*H*$_3$). $^{13}C\{^1H\}$ NMR ($CDCl_3$, ppm): 160.45 (C), 157.68 (CH), 152.02 (C), 129.73 (CH), 115.19 (CH), 110.16 (CH),108.01(CH), 54.92 (CH_3). Calc. for $C_{60}H_{60}Mo_2N_8O_8$ (*MW* = 1213.04): C, 59.40; H, 4.98; N, 9.24%;

Table 1
Crystal data for compounds **1**–**3**

Compound	**1**	**2a**	**2b**	**3**
Formula	$C_{60}H_{60}Mo_2N_8O_8$	$C_{41}H_{47}B_2Cl_2F_8Mo_2N_9O_4$	$C_{39.5}H_{44.5}B_2ClF_8Mo_2N_{8.5}$	$C_{64}H_{72}Mo_4N_8O_{12}$
Fw	1213.04	1166.28	1103.29	1529.06
Crystal system	Monoclinic	Triclinic	Triclinic	Triclinic
Space group	$P2_1/n$	$P\bar{1}$	$P\bar{1}$	$P\bar{1}$
A, Å	15.9394(8)	11.6403(9)	13.0132(7)	8.7284(8)
B, Å	9.8710(5)	12.3965(10)	19.5509(10)	12.5187(11)
C, Å	18.2809(10)	18.9062(13)	22.4735(12)	15.325(4)
α, °	90	103.426(5)	96.721(1)	103.059(12)
β, °	106.415(1)	103.615(5)	106.810(1)	100.854(12)
γ, °	90	97.719(7)	107.319(1)	96.747(7)
V, Å^3	2759.0(2)	2527.0(3)	5094.5(5)	1579.5(4)
Z	2	2	4	1
$d_{calc.}$, g/cm^3	1.460	1.533	1.438	1.608
$F(000)$	1248	1176	2224	776
Cryst. size, mm	0.44 × 0.48 × 0.74	0.2 × 0.6 × 0.8	0.3 × 0.4 × 0.4	0.1 × 0.4 × 0.4
μ(Mo Kα), mm^{-1}	0.518	0.680	0.619	0.844
reflections collected	10605	10104	24790	6637
Independent reflections	4774 [R(int) = 0.0288]	8734 [R(int) = 0.0246]	16984 [R(int) = 0.0362]	5487 [R(int) = 0.0316]
Data/restraints/parameters	4774/0/472	8734/0/613	16984/6/1183	5487/0/474
Quality-of-fit indicator[c]	1.091	1.046	1.024	1.039
final R indices $[I > 2\sigma(I)]$[a,b]	$R_1 = 0.0278$ $wR_2 = 0.0749$	$R_1 = 0.0615$ $wR_2 = 0.1670$	$R_1 = 0.0694$ $wR_2 = 0.1526$	$R_1 = 0.0529$ $wR_2 = 0.1231$
R indices (all data)	$R_1 = 0.0293$ $wR_2 = 0.0767$	$R_1 = 0.0725$ $wR_2 = 0.1785$	$R_1 = 0.0819$ $wR_2 = 0.1616$	$R_1 = 0.0821$ $wR_2 = 0.1388$
Largest diff. peak and hole, e/Å^3	0.319 and −0.495	1.118 and −1.344	1.464 and −0.646	1.001 and −0.838

[a] $R_1 = \Sigma||F_o| - |F_c||/\Sigma|F_o|$.

[b] $wR_2 = [\Sigma w(F_o^2 - F_c^2)^2/\Sigma w(F_o^2)^2]^{1/2}.w = 1/[\sigma^2(F_o^2) + (ap)^2 + (bp)]$, $p = [\max(F_o^2 \text{ or } 0) + 2(F_c^2)]/3$. $a = 0.0369$, $b = 1.4931$, **1**; $a = 0.1022$, $b = 5.5102$, **2a**; $a = 0.0315$, $b = 26.2974$, **2b**; $a = 0.0566$, $b = 5.0489$, **3**.

[c] Quality-of-fit = $[\Sigma w(|F_o^2| - |F_c^2|)^2/N_{observed} - -N_{parameters})]^{1/2}$.

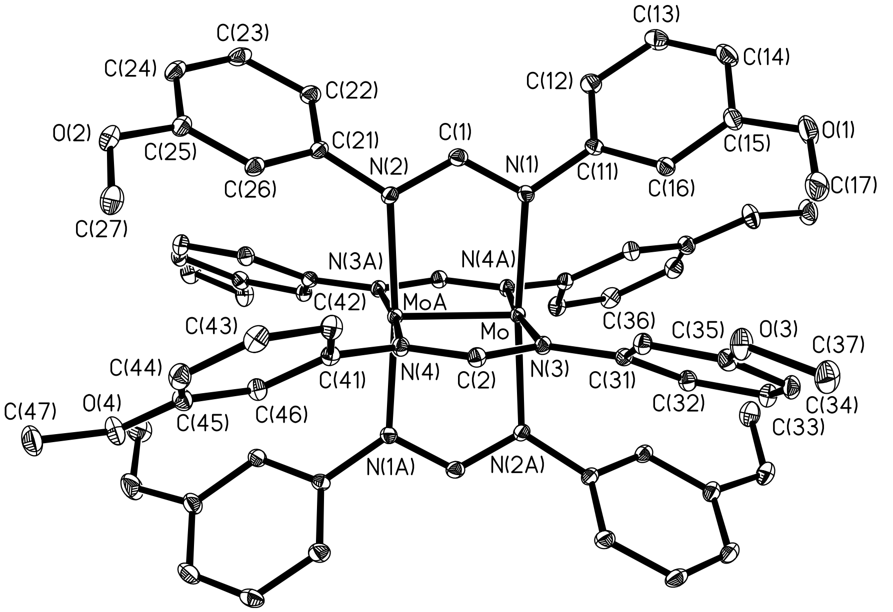

Fig. 1. ORTEP drawing for complex **1**. Thermal ellipsoids shown at 20% probability level.

Found: C, 58.97; H, 5.10; N, 8.99%. IR (KBr disk): 2938(w), 2834(w), 2360(w), 1648(w), 1599(s), 1583(s), 1538(s), 1482(s), 1326(m), 1282(m), 1258(m), 1195(m), 1151(s), 1085(w), 1040(m), 984(w), 940(w), 850(m), 772(m), 695(m), 633(w), 510(w), 449(w). Crystals suitable for X-ray crystallography were obtained by diffusion of CH_3OH into a CH_2Cl_2 solution of the yellow product.

2.4. Preparation of cis-[$Mo_2(DmAniF)_2(CH_3CN)_4$][BF_4]$_2$ (**2**)

$Mo_2(DmAniF)_4$ (0.25 g, 0.20 mmol) and Me_3OBF_4 (0.18 g, 1.20 mmol) were placed in a flask containing 10 mL CH_3CN. The mixture was stirred for 5 h to yield a red solution and 20 mL diethyl ether was then added to give a red solid. The solid was filtered, washed by diethyl ether and then dried under reduced pressure to give the red product. Yield: 0.16 g (78%). UV–vis: 475 nm (CH_2Cl_2, $\varepsilon = 1196$ $M^{-1}cm^{-1}$). ^1H NMR ($CDCl_3$, ppm): 8.81 (s, 2H, C*H*), 6.98 (t, 4H, H^{meta}), 6.58 (d, 4H, H^{para}), 6.21 (s, 4H, H^{ortho}), 6.15 (d, 4H, H^{ortho}), 3.52 (s, 12H, OCH_3), 1.98 (s, 12H, CH_3). $^{13}C\{^1H\}$ NMR ($CDCl_3$, ppm): 161.00 (C), 160.58 (CH), 148.04 (C), 130.34 (CH), 114.64 (CH), 114.02 (C), 111.85 (CH), 107.88 (CH), 55.16 (CH_3), 3.76 (CH_3). Calc. for $C_{38}H_{42}B_2F_8Mo_2N_8O_4$ (MW = 1040.29): C, 43.87; H, 4.07; N, 10.77%; Found: C, 43.49; H, 4.25; N, 11.02%. IR (KBr disk): 2939(w), 2838(w), 1687(s), 1594(s), 1532(m), 1492(m), 1464(m), 1435(w), 1384(w), 1330 (m), 1285(m), 1264(m), 1196(w), 1155(s), 1117(s), 1085(s), 1037(s), 936(w), 846(w), 771(m), 686(w), 533(w), 522(w), 457(w). Crystals of **2a** suitable for X-ray crystallography were obtained by diffusion of diethyl ether into a CH_2Cl_2 solution

Table 2
Selected bond distances Å and Angles ° for **1**

Bond distances			
Mo–Mo(A)	2.1023(3)	Mo–N(2A)	2.1570(18)
Mo–N(4A)	2.1644(18)	Mo–N(1)	2.1650(18)
Mo–N(3)	2.1671(18)	O(1)–C(15)	1.365(3)
Bond angles			
Mo(A)–Mo–N(2A)	92.61(5)	Mo(A)–Mo–N(4A)	92.40(5)
N(2A)–Mo–N(4A)	91.09(7)	Mo(A)–Mo–N(1)	92.72(5)
N(2A)–Mo–N(1)	174.66(7)	N(4A)–Mo–N(1)	89.06(7)
Mo(A)–Mo–N(3)	93.18(5)	N(2A)–Mo–N(3)	88.27(7)
N(4A)–Mo–N(3)	174.42(7)	N(1)–Mo–N(3)	91.06(7)

Symmetry transformations used to generate equivalent atoms: (A) $-x+2$, $-y+1$, $-z$.

Table 3
Selected bond distances (Å) and angles (°) for **2a**

Bond distances			
Mo(1)–Mo(2)	2.1286(6)	Mo(1)–N(1)	2.100(4)
Mo(1)–N(3)	2.099(5)	Mo(1)–N(5)	2.174(5)
Mo(1)–N(6)	2.177(5)	Mo(2)–N(2)	2.117(4)
Mo(2)–N(4)	2.123(4)	Mo(2)–N(7)	2.173(5)
Mo(2)–N(8)	2.178(5)	Mo(2)···F(1A)	2.685(4)
Bond angles			
N(3)–Mo(1)–N(1)	95.29(18)	N(3)–Mo(1)–Mo(2)	92.78(11)
N(1)–Mo(1)–Mo(2)	92.68(11)	N(3)–Mo(1)–N(5)	88.66(19)
N(1)–Mo(1)–N(5)	163.20(17)	Mo(2)–Mo(1)–N(5)	103.45(12)
N(3)–Mo(1)–N(6)	160.09(17)	N(1)–Mo(1)–N(6)	91.95(19)
Mo(2)–Mo(1)–N(6)	105.41(12)	N(5)–Mo(1)–N(6)	79.40(19)
N(2)–Mo(2)–N(4)	96.05(18)	N(2)–Mo(2)–Mo(1)	91.54(11)
N(4)–Mo(2)–Mo(1)	91.47(11)	N(2)–Mo(2)–N(7)	166.07 (17)
N(4)–Mo(2)–N(7)	90.08(18)	Mo(1)–Mo(2)–N(7)	100.82(12)
N(2)–Mo(2)–N(8)	88.61(18)	N(4)–Mo(2)–N(8)	165.82(17)
Mo(1)–Mo(2)–N(8)	101.82(12)	N(7)–Mo(2)–N(8)	82.63(19)

Symmetry transformations used to generate equivalent atoms: (A) $x-1$, y, z.

Table 4
Selected bond distances (Å) and angles (°) for **2b**

Bond distances			
Mo(1)–N(3)	2.106(5)	Mo(1)–N(1)	2.113(5)
Mo(1)–Mo(2)	2.1432(8)	Mo(1)–N(5)	2.187(6)
Mo(1)–N(6)	2.191(6)	Mo(2)–N(2)	2.097(5)
Mo(2)–N(4)	2.100(5)	Mo(2)–N(8)	2.178(6)
Mo(2)–N(7)	2.184(6)	Mo(3)–N(9)	2.099(5)
Mo(3)–N(11)	2.110(5)	Mo(3)–Mo(4)	2.1317(9)
Mo(3)–N(13)	2.154(7)	Mo(3)–N(14)	2.184(6)
Mo(4)–N(12)	2.103(5)	Mo(4)–N(10)	2.110(5)
Mo(4)–N(16)	2.170(6)	Mo(4)–N(15)	2.190(6)
Bond angles			
N(3)–Mo(1)–N(1)	95.3(2)	N(3)–Mo(1)–Mo(2)	91.81(14)
N(1)–Mo(1)–Mo(2)	91.14(14)	N(3)–Mo(1)–N(5)	167.8(2)
N(1)–Mo(1)–N(5)	89.5(2)	Mo(2)–Mo(1)–N(5)	99.30(15)
N(3)–Mo(1)–N(6)	87.9(2)	N(1)–Mo(1)–N(6)	166.6(2)
Mo(2)–Mo(1)–N(6)	101.81(16)	N(5)–Mo(1)–N(6)	85.0(2)
N(2)–Mo(2)–N(4)	95.3(2)	N(2)–Mo(2)–Mo(1)	92.95(14)
N(4)–Mo(2)–Mo(1)	92.08(14)	N(2)–Mo(2)–N(8)	164.0(2)
N(4)–Mo(2)–N(8)	90.3(2)	Mo(1)–Mo(2)–N(8)	101.82(16)
N(2)–Mo(2)–N(7)	85.1(2)	N(4)–Mo(2)–N(7)	163.1(2)
Mo(1)–Mo(2)–N(7)	104.79(15)	N(8)–Mo(2)–N(7)	85.3(2)
N(9)–Mo(3)–N(11)	95.6(2)	N(9)–Mo(3)–Mo(4)	91.30(16)
N(11)–Mo(3)–Mo(4)	92.15(15)	N(9)–Mo(3)–N(13)	86.3(2)
N(11)–Mo(3)–N(13)	163.8(3)	Mo(4)–Mo(3)–N(13)	104.0(2)
N(9)–Mo(3)–N(14)	165.8(3)	N(11)–Mo(3)–N(14)	89.1(2)
Mo(4)–Mo(3)–N(14)	101.94(18)	N(13)–Mo(3)–N(14)	85.5(2)
N(12)–Mo(4)–N(10)	95.5(2)	N(12)–Mo(4)–Mo(3)	91.72(15)
N(10)–Mo(4)–Mo(3)	92.85(15)	N(12)–Mo(4)–N(16)	87.4(2)
N(10)–Mo(4)–N(16)	163.2(2)	Mo(3)–Mo(4)–N(16)	103.63(18)
N(12)–Mo(4)–N(15)	164.9(2)	N(10)–Mo(4)–N(15)	90.3(2)
Mo(3)–Mo(4)–N(15)	101.85(19)	N(16)–Mo(4)–N(15)	83.1(2)

of the red product, while crystals of **2b** were obtained by diffusion of diethyl ether into a CH_2Cl_2/CH_3CN (CH_2Cl_2: CH_3CN = 9: 1) solution of the red product.

2.5. Preparations of *cis*-$[Mo_2(DmAniF)_2]_2(\mu\text{-}OCH_3)_4$ (3)

Method A: *cis*-$[Mo_2(DmAniF)_2(CH_3CN)_4][BF_4]_2$ (0.42 g, 0.40 mmol) and $NaOCH_3$ (0.18 g, 1.00 mmol) were placed in a flask containing 40 mL CH_3OH. The mixture was stirred for 3 h to yield a red solution and then 60 mL diethyl ether was added to give a red solid. The solid was filtered, washed with methanol and diethyl ether and then dried under reduced pressure to give a brown product. The brown product in 20 mL CH_2Cl_2 was passed through a Celite-packed frit, and then 80 mL CH_3OH was added to give a red solid. The solid was filtered, washed with methanol and diethyl ether and then dried under reduced pressure to give a red product. Crystals suitable for X-ray crystallography were obtained by diffusion of CH_2Cl_2 into a CH_3OH solution of the red product. Yield: 0.26 g (41%). UV–vis: 498 nm (CH_2Cl_2). Calc. for $Mo_4O_{13}N_8C_{65}H_{76}$ (**3**·CH_3OH, $MW = 1568.17$): C, 49.74; H, 4.88; N, 7.18%; Found: C, 49.48; H, 5.03; N, 6.69%.

Method B: HDmAniF (0.11 g, 0.42 mmol) and $[Mo_2(CH_3CN)_{10}][BF_4]_4$ (0.20 g, 0.21 mmol) was placed in a flask containing 10 mL CH_3CN. The mixture was stirred for 8 h under N_2 to yield a red solution. Then dry red solution and add 20 ml diethyl ether wash product. The solid was filtered, washed by diethyl ether and then dried under reduced pressure to give the red product. Crystals suitable for X-ray crystallography were obtained by diffusion CH_2Cl_2 into a CH_3OH solution of the red product. Yield: 0.08 g (25%).

3. X-ray crystallography

The diffraction data of **1**–**3** were collected on a Siemens CCD or a Bruker AXS diffractometer, which were equipped

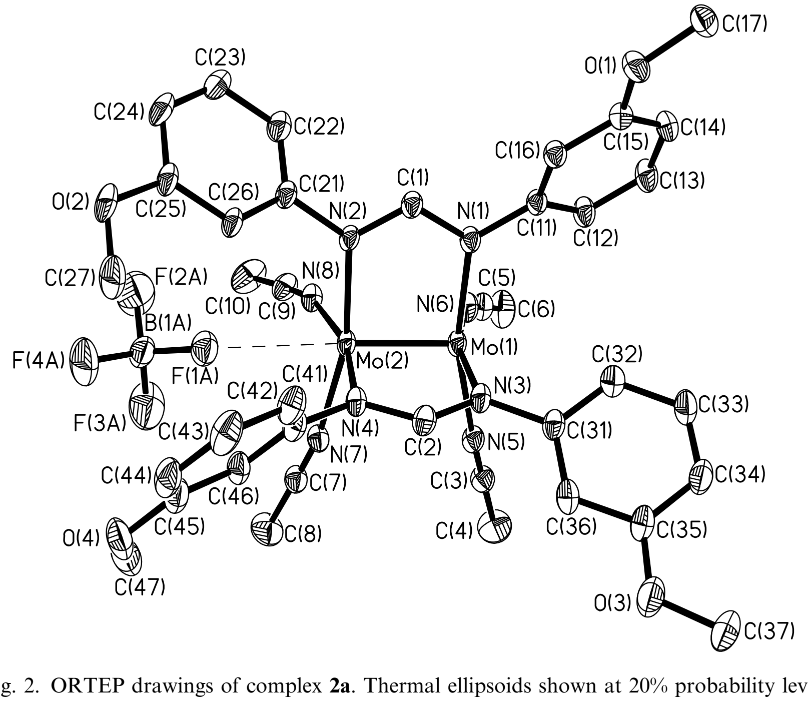

Fig. 2. ORTEP drawings of complex **2a**. Thermal ellipsoids shown at 20% probability level.

Table 5
Structural data of selected dimolybdenum complexes with $Mo_2(\mu_2\text{-}L)_2(CH_3CN)_4$

Complex	Mo–Mo (Å)	Mo···(ax) (Å)	Reference
cis- $[Mo_2(DphF)_2(CH_3CN)_4(ax\text{-}CH_3CN)][BF_4]_2$[a]	2.1457(7)	2.595(3)	[4a]
cis-$[Mo_2(DpAniF)_2(CH_3CN)_4(ax\text{-}CH_3CN)][BF_4]_2$[b]	2.1439(6)	2.590(4)	[4b]
trans-$[Mo_2(H_2DMepyF)_2(CH_3CN)_4(ax\text{-}CH_3CN)_2][BF_4]_6$[c]	2.1504(6)	2.635(5)	[13]
trans-$[Mo_2(H_2DMepyF)_2(CH_3CN)_4][ax\text{-}BF_4]_2[BF_4]_4$[c]	2.1321(6)	2.592(2)	[13]
cis-$[Mo_2(HDpyF)_2(CH_3CN)_4](BF_4)_4$[d]	2.1348(8)	–	[14]
cis-$[Mo(DmAniF)_2(CH_3CN)_4][ax\text{-}BF_4][BF_4]$ (**2a**)	2.1286(6)	2.685(4)	This work
cis-$[Mo(DmAniF)_2(CH_3CN)_4][BF_4]_2$ (**2b**)	2.1317(9)	–	This work
cis-$[Mo(DmAniF)_2(CH_3CN)_4(ax\text{-}CH_3CN)][BF_4]_2$ (**2b**)	2.1432(8)	2.692(8)	This work

[a] $phF^- = N,N'$-diphenylformamidine anion.
[b] $DpAniF^- = N,N'$-di(4-methoxyphenyl)formamidine anion.
[c] $H_2DMepyF^+ = N,N'$-di(6-methyl-2-pyridyl)formamidine cation.
[d] $HDpyF = N,N'$-di (2-pyridyl)formamidine.

with a graphite-monochromated MoK_α ($\lambda_\alpha = 0.71073$ Å) radiation. Data reduction was carried by standard methods with use of well-established computational procedures [9].

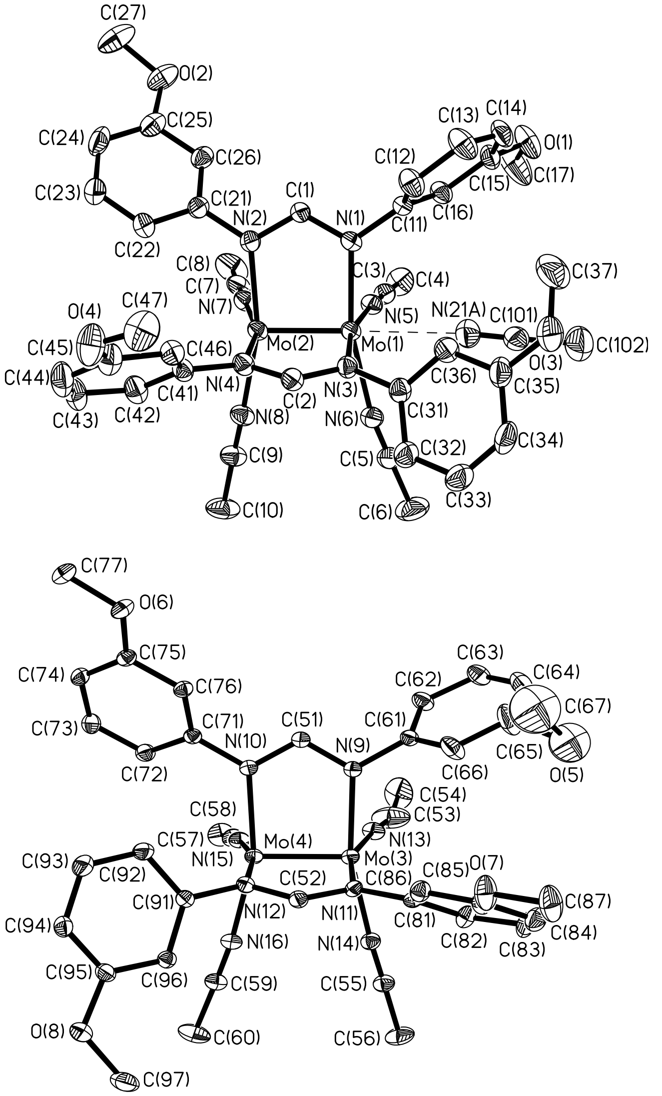

Fig. 3. ORTEP drawings of the two independent molecules of complex **2b**. The top molecule shows axial Mo···N interaction through CH_3CN molecule. Thermal ellipsoids shown at 20% probability level.

A red crystal of **1** was mounted on the top of a glass fiber with epoxy cement. Hemisphere data collection method was used to scan the data points at $4.92 < 2\theta < 50.02°$. The structure factors were obtained after Lorentz and polarization corrections. The positions of some of the heavier atoms were located by direct methods. The remaining atoms were found from a series of alternating difference Fourier maps and least-square refinements. The final residuals of the refinement were $R_1 = 0.0278$ and $wR_2 = 0.0749$. The X-ray crystallographic procedures for **2** and **3** were similar to those for **1**. Basic information pertaining to crystal parameters and structure refinement is summarized in Table 1.

4. Results and discussion

4.1. Syntheses

The yellow complex $Mo_2(DmAniF)_4$, **1**, was prepared by reaction of $Mo(CO)_6$ with excess HDmAniF in *o*-dichlorobenzene, whereas the reaction of **1** with excess Me_3OBF_4 in CH_3CN afforded *cis*-$[Mo_2(DmAniF)_2(CH_3CN)_4](BF_4)_2$, **2**. Reaction of **2** with $NaOCH_3$ in CH_3OH produced the tetranuclear complex *cis*-$[Mo_2(DmAniF)_2]_2(\mu\text{-}OCH_3)_4$, **3**, which can also be prepared by reacting *m*-HDMophF with $[Mo_2(CH_3CN)_{10}][BF_4]_4$ in CH_3CN.

4.2. Structures of *1*

Yellow crystals of **1** conform to the space group $P2_1/n$ with two molecules in a unit cell. Fig. 1 shows the ORTEP diagram for **1**. Selected bond distances and angles are listed in Table 2. The molecular structure of **1** consists of two molybdenum atoms [Mo–Mo = 2.1023(3) Å] which are spanned by four $DmAniF^-$ ligands. Its structure reveals that the four ligands bridge the two metal centers through the two nitrogen atoms, resulting in the *s-cis*, *s-trans* and *s-trans*, *s-trans* conformations. The ligands of complex **1** are not flat, but twisted around the C–N bonds, with dihedral angles (between the planes of the two anisole rings) of 35.8° for the ligands with *s-cis*, *s-trans* conformation and 42.3° for those with *s-trans*, *s-trans* conformation.

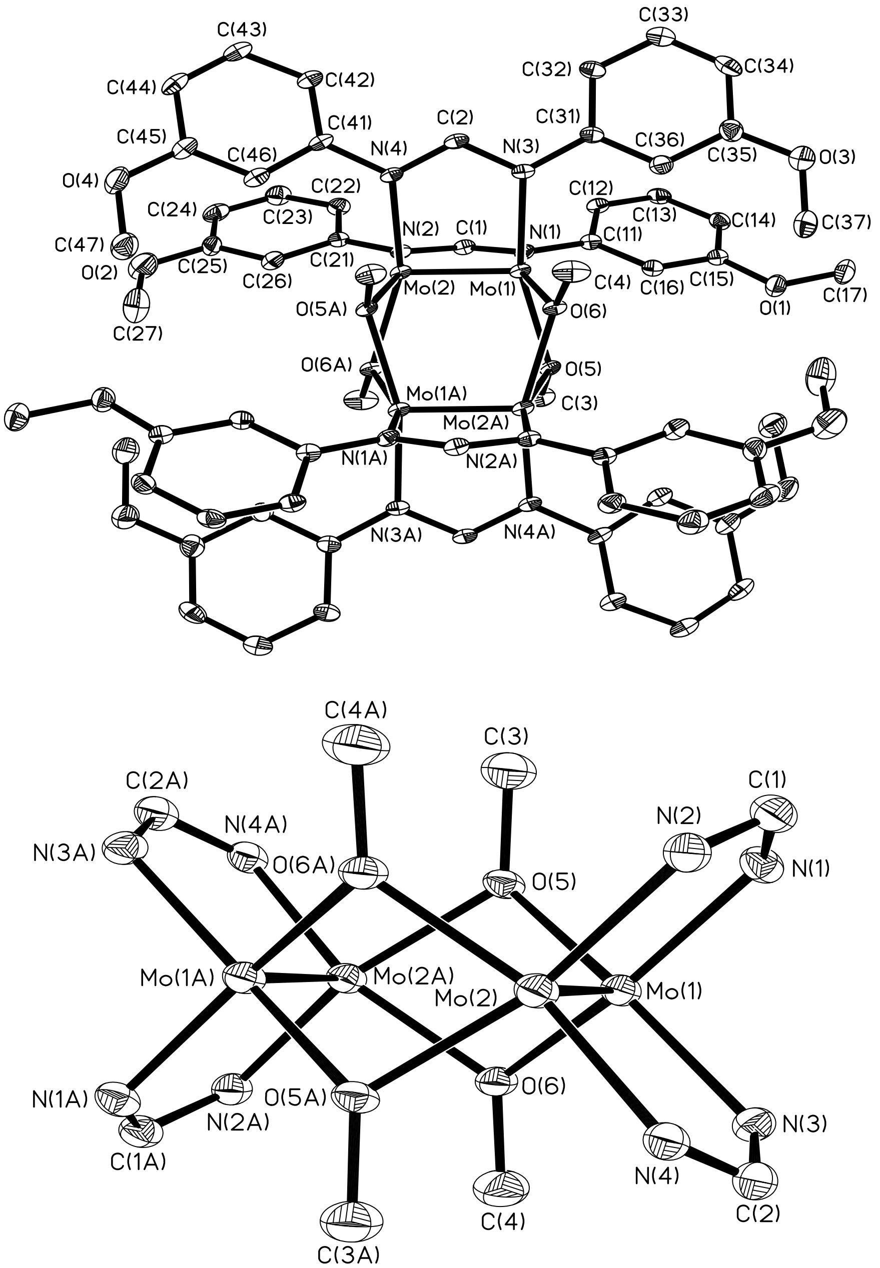

Fig. 4. ORTEP drawing for complex **3** (top) and its core structure (bottom). Thermal ellipsoids shown at 20% probability level.

Three other dinuclear paddlewheel complexes containing four DmAniF^{-} ligands have been reported, which are $Rh_2(DmAniF)_4$ [10], $Cr_2(DmAniF)_4$ [11] and $W_2(DmAniF)_4$ [12]. An investigation into the ligand conformations of these complexes shows that all the four ligands of the Rh complex adopt the *s-trans*, *s-trans* conformation, while those in the Cr and W complexes adopt, similar to complex **1**, the *s-cis*, *s-trans* and *s-trans*, *s-trans* conformations. It is also noted that while the isomeric complex $Mo_2(DpAniF)_4$ [2b] [Mo–Mo = 2.0964 (5) Å] has been structurally characterized, the other isomeric complex $Mo_2(DoAniF)_4$ has not been reported, although several dimolybdenum complexes of the types $Mo_2(O_2CCH_3)_3(DoAniF)$, *trans*-$Mo_2(O_2CR)_2(DoAniF)_2$ (R=CH_3, CF_3, and Pr^{n}) and $Mo_2(O_2CCH_3)(DoAniF)Cl_2(PMe_3)_2$ [5g] and the mixed ligand complexes [5h] *trans*-$Mo_2(O_2CCH_3)(DpyF)(DoAniF)_2$, *trans*-$Mo_2(O_2CCH_3)(DpmF)(DoAniF)_2$, *trans*-$Mo_2(O_2CCH_3)(DMepyF)(DoAniF)_2$, *trans*-$Mo_2(O_2CCH_3)(DMepyF)_2(DoAniF)$, and *trans*-$Mo_2(DMepyF)_2(DoAniF)_2$ have been structurally characterized.

4.3. Structures of 2

The red complex **2** crystallized in two different forms, **2**·CH_2Cl_2·CH_3CN, **2a**, and **2**·0.5CH_2Cl_2·0.5CH_3CN, **2b**, and both conform to the space group P$\bar{1}$. Figs. 2 and 3 shows the ORTEP diagrams for the complexes **2a**, and **2b**, respectively, and Tables 3 and 4 list the selected bond distances and angles for complexes **2a** and **2b**, respectively. The two dimolybdenum centers of both **2a** and **2b** are coordinated by two *cis* DmAniF$^-$ ligands and four CH_3CN ligands. The Mo–Mo distances in **2a** is 2.1281(6) which is normal for dinuclear complexes with Mo–Mo quadruple bonds. It is also seen that while one of the two BF_4^- anions coordinates to the Mo–Mo axial site through the fluoride atom [Mo···F = 2.685 (4) Å], the other BF_4^- anion interacts with the cation through C–H···F hydrogen bonds (H···F = 2.452 Å; ∠ C–H···F = 147.9°). The two *cis* DmAniF$^-$ ligands adopt the *s-cis*, *s-trans* conformation and each twists around the C–N bonds, with a dihedral angle between the planes of the two anisole rings of 72.2 and 98.9°, respectively.

Complex **2b** contains two independent molecules as shown in Fig. 3. The top molecule [Mo–Mo = 2.1432(8) Å] in Fig. 3 shows axial interaction by CH_3CN [Mo···N = 2.692 (8) Å] and the two *cis* DmAniF$^-$ ligands adopt the same *s-cis*, *s-trans* conformation, while the bottom one [Mo–Mo = 2.1317(9) Å] shows no axial interaction and the two *cis* DmAniF$^-$ ligands adopt different conformations, which are *s-cis*, *s-trans* and *s-cis*, *s-cis*, respectively. The dihedral angles between the planes of the two anisole rings of the two bidentate *cis* DmAniF$^-$ ligands are 84.8 and 87.8° for the top molecule and 89.1 and 88.5° for the bottom one, respectively.

Table 5 lists the structural data for dimolybdenum complexes with $Mo_2(\mu_2\text{-}L)_2(CH_3CN)_4$ core, where L is the anionic, cationic or neutral form of a formamidine ligand. It is seen that the Mo–Mo distance of **2a**, 2.1286(6) Å, is the shortest among the compounds having $Mo_2(\mu_2\text{-}L)_2(CH_3CN)_4$ core. In the two independent molecules of **2b**, the one with axial interaction through CH_3CN molecule shows longer Mo–Mo distance than the one with no axial interaction.

Table 6
Selected Bond Distances (Å) and Angles (°) for **3**

Bond distances			
Mo(1)–N(1)	2.107(5)	Mo(1)–Mo(2)	2.1185(10)
Mo(1)–O(6)	2.129(4)	Mo(1)–N(3)	2.130(5)
Mo(1)–O(5)	2.139(4)	Mo(2)–N(4)	2.109(5)
Mo(2)–O(5A)	2.128(4)	Mo(2)–O(6A)	2.128(4)
Mo(2)–N(2)	2.137(5)	O(5)–Mo(2A)	2.128(4)
O(6)–Mo(2A)	2.128(4)		
Bond angles			
N(1)–Mo(1)–Mo(2)	92.84(16)	N(1)–Mo(1)–O(6)	159.38(19)
Mo(2)–Mo(1)–O(6)	105.14(13)	N(1)–Mo(1)–N(3)	93.7(2)
Mo(2)–Mo(1)–N(3)	92.06(17)	O(6)–Mo(1)–N(3)	95.61(18)
N(1)–Mo(1)–O(5)	92.99(18)	Mo(2)–Mo(1)–O(5)	103.69(12)
O(6)–Mo(1)–O(5)	73.24(15)	N(3)–Mo(1)–O(5)	162.5(2)
N(4)–Mo(2)–Mo(1)	92.76(17)	N(4)–Mo(2)–O(5A)	92.96(18)
Mo(1)–Mo(2)–O(5A)	103.97(12)	N(4)–Mo(2)–O(6A)	159.4(2)
Mo(1)–Mo(2)–O(6A)	105.35(13)	O(5A)–Mo(2)–O(6A)	73.47(16)
N(4)–Mo(2)–N(2)	94.5(2)	Mo(1)–Mo(2)–N(2)	91.89(16)
O(5A)–Mo(2)–N(2)	162.1(2)	O(6A)–Mo(2)–N(2)	94.64(18)
C(3)–O(5)–Mo(2A)	127.3(4)	C(3)–O(5)–Mo(1)	122.9(4)
Mo(2A)–O(5)–Mo(1)	99.08(16)	C(4)–O(6)–Mo(2A)	128.9(5)
C(4)–O(6)–Mo(1)	128.9(5)	Mo(2A)–O(6)–Mo(1)	99.38(17)

4.4. Structure of 3

Red crystals of **3** conform to the space group $P\bar{1}$ with one molecule in a unit cell. Fig. 4 shows the ORTEP drawing for **3** (top) and its core structure (bottom) and Table 6 lists the selected bond distances and angles. The molecule bears four bridging CH_3O^- that link two quadruply bonded moieties which are also bridged by two *cis* DmAniF$^-$ ligands. The Mo–Mo distance of 2.1185(10) Å is consistent with the presence of a quadruply bonded Mo_2^{4+} unit. The long Mo···Mo distances are 3.2463(8) Å, which is well outside of bonding range. The Mo–O distances are in the range from 2.128(4) to 2.139(4) Å and the Mo–O–Mo angles are 99.08 (16) and 99.38 (17)°. The two DmAniF$^-$ ligands which adopt the same *s-trans*, *s-trans* conformation are not flat, but twisted around the C–N bonds, with dihedral angles of 10.7 and 22.1°, respectively.

Complex **3** makes interesting comparisons with the similar complexes of the type $[Mo_2(NN)_2]_2(\mu\text{-}X)_4$ (NN=*N*,*N*′-di(4-methoxyphenyl) formamidine anion, X=Cl, I, OCH_3, OC_2H_5; NN=*N*,*N*′-di(4-methylphenyl)formamidine anion, X=Cl; NN=*N*,*N*′-di(4-fluorophenyl)formamidine anion, X=Cl), and $[Mo_2I_2(PBu^n_3)_2]_2(\mu - I)_4$, where the two dimolybdenum units are linked by the halide atoms or alkoxide groups, as shown in Chart 1 [15,16]. Table 7 lists some selected structural data for these complexes. It is seen that while the long Mo···Mo distances of these complexes are sensitive to the natures of the bridging ligands, those of the short quadruple-bonded Mo–Mo distances fall in the small range 2.117(1)–2.1317(7). Although the Mo···Mo and Mo–O distances and Mo–O–Mo angles of **3** and $[Mo_2(DpAniF)_2]_2(\mu\text{-}OMe)_4$ are about the same, the Mo–Mo distance of **3** is significantly shorter than that of $[Mo_2(DpAniF)_2]_2(\mu\text{-}OMe)_4$. Also noted is that those bridged by the halide atoms show longer Mo···Mo nonbonded distances, presumably due to the larger atomic sizes of the halide atoms.

4.5. Magnetic anisotropy

It has been shown that the chemical shifts of the protons in the vicinity of the dimolybdenum core are sensitive to the magnetic anisotropy ($\Delta\chi$) from the metal–metal multiple bond and $\Delta\chi$ can be estimated on the basis of the δ of methine proton (–NCHN–) of the formamidinate group according to the following equation [2]:

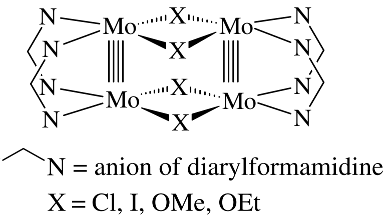

Chart 1. The structure of the $[Mo_2(NN)_2]_2(\mu\text{-}X)_4$ core.

Table 7
Selected bond distances (Å) and angles (°) for some $[Mo_2(NN)_2]_2(\mu\text{- }X)_4$ complexes and $[Mo_2I_2(PBu^n_3)_2]_2(\mu - I)_4$

Complex	Mo–Mo	Mo···Mo	Mo–X	Mo–X–Mo	Ref.
$[Mo_2(DpAniF)_2]_2(\mu\text{-}Cl)_4$[a]	2.1191(4)	3.602(1)	2.516[2][d]	91.42[5]	[15]
$[Mo_2(DTolF)_2]_2(\mu\text{-}Cl)_4$[b]	2.118(1)	3.592(1)	2.513[1]	91.25[5]	[15]
$[Mo_2(DPh^fF)_2]_2(\mu\text{-}Cl)_4$[c]	2.123(1)	3.563(1)	2.510[2]	90.44[5]	[15]
$[Mo_2(DpAniF)_2]_2(\mu\text{-}I)_4$	2.117(1)	3.915(1)	2.845[2]	87.02[2]	[15]
$[Mo_2I_2(PBu^n_3)_2]_2(\mu - I)_4$	2.129[3]	3.998[3]	2.794[2]	90.57[5]	[15]
$[Mo_2(DpAniF)_2]_2(\mu\text{-}OMe)_4$	2.1315(7)	3.245	2.142[4]	98.55[16]	[16]
$[Mo_2(DpAniF)_2]_2(\mu\text{-}OEt)_4$	2.1317(7)	3.241	2.136[2]	98.67[9]	[16]
3	2.1185(10)	3.2463(8)	2.131[4]	99.23[17]	This work

[a] DpAniF = *N*,*N*′-di(4-methoxyphenyl)formamidine anion.

[b] DTolF = *N*,*N*′-di(4-methylphenyl)formamidine anion.

[c] DPh^fF = *N*,*N*′-di(4-fluorophenyl)formamidine anion.

[d] Brackets in standard errors indicate that the value given has been averaged.

$$\Delta\chi = 12\pi r^3\Delta\delta/(1 - 3cos^2\theta)$$

where $\Delta\delta$ is the change of the chemical shift due to the magnetic anisotropy which is best referenced to the dinickel analogs $Ni_2(form)_4$, r is the calculated distance of the methine proton from the center of the Mo–Mo bond and θ is the angle between the r vector and the Mo–Mo vector. According to this equation, the $\Delta\chi$ of complex **1** is calculated as $4920 \pm 17 \times 10^{-34}$ m^3/molecule. The magnetic anisotropy can also be calculated using the equation related to the Hammett constant σ: $\Delta\chi = 5000 \times 10^{-34}$ m^3/molecule-$8\sigma\rho$ [12], where ρ is the reaction constant and for complexes of the type Mo_2(formamidine)$_4$, its value is 38.991×10^{-34} m^3/molecule. Substituting the Hammett constant which is 0.12 for the *m*-$DMophF^-$ ligand, the $\Delta\chi$ of complex **1** is calculated as 4963×10^{-34} m^3/molecule. These two values, $4920 \pm 17 \times 10^{-34}$ m^3/molecule and 4963×10^{-34} m^3/molecule, are similar to the one, 5040×10^{-34} m^3/molecule reported by Ren and coauthors [2b].

5. Concluding remarks

The syntheses and structurally characterization of the dinuclear complexes $Mo_2(DmAniF)_4$, **1** and *cis*-$[Mo_2(DmAniF)_2(CH_3CN)_4][BF_4]_2$, **2**, and a tetranuclear complex *cis*-$[Mo_2(DmAniF)_2]_2(\mu\text{-}OCH_3)_4$, **3**, which contain bridging anions of *N*,*N*′-di(3-methoxyphenyl)formamidine have been successfully accomplished. The Mo–Mo distance in $\mathbf{2} \cdot CH_2Cl_2{\cdot}CH_3CN$, 2.1281(6) Å, is the shortest among the compounds having $Mo_2(\mu_2\text{-}L)_2(CH_3CN)_4$ core, where L is the anionic, cationic or neutral form of a formamidine ligand Several conformations of the $DmAniF^-$ anion such as *s-cis*, *s-trans*, *s-cis*, *s-cis* and *s-trans*, *s-trans* have been observed, which demonstrate that this ligand is sufficiently flexible to accommodate the solid state structures of these complexes.

6. Supplementary material

Crystallographic data (excluding structure factors) for the structures in this paper has been deposited with the Cambridge Crystallographic Data Centre as supplementary publication numbers CCDC 665671–665674. Copies of the data can be obtained, free of charge, on application to CCDC, 12 Union Road, Cambridge CB2 1EZ, UK [Fax: +44(0) 1223 336033 or e-mail: deposit@ccdc.cam.ac.uk].

Acknowledgement

We wish to thank the National Science Council of the Republic of China for support.

References

[1] F.A. Cotton, C.A. Murillo, R.A. Walton, Multiple Bonds between Metal Atoms, Springer Science and Business Media, Inc., New York, 2005.

[2] (a) C. Lin, J.D. Protasiewics, T. Ren, Inorg. Chem. 35 (1996) 7455;
(b) C. Lin, J.D. Protasiewicz, E.T. Smith, T. Ren, Inorg. Chem. 35 (1996) 6422.

[3] R. Clérac, F.A. Cotton, K.R. Dunbar, C.A. Murillo, X. Wang, Inorg. Chem. 40 (2001) 420.

[4] (a) F.A. Cotton, L.M. Daniels IV, G.T. Jordan, C. Lin, C.A. Murillo, J. Am. Chem. Soc. 120 (1998) 3398;
(b) M.H. Chisholm, F.A. Cotton, L.M. Daniels, K. Folting, J.C. Huffman, S.S. Iyer, C. Lin, A.M. Macintosh, C.A. Murillo, J. Chem. Soc., Dalton Trans. (1999) 1387;
(c) F.A. Cotton, J.P. Donahue, C. Lin, C.A. Murillo, Inorg. Chem. 40 (2001) 1234;
(d) F.A. Cotton, J.P. Donahue, C.A. Murillo, Inorg. Chem. 40 (2001) 2229;
(e) F.A. Cotton, C. Lin, C.A. Murillo, Inorg. Chem. 40 (2001) 575;
(f) F.A. Cotton, C. Lin, C.A. Murillo, Inorg. Chem. 40 (2001) 478;
(g) F.A. Cotton, L.M. Daniels, C. Lin, C.A. Murillo, Chem. Commun. (1999) 841.

[5] (a) S.J. Archibald, N.W. Alcock, D.H. Busch, D.R. Whitcomb, Inorg. Chem. 38 (1999) 5571;
(b) S. Radak, Y. Ni, G. Xu, K.L. Shaffer, T. Ren, Inorg. Chim. Acta 321 (2001) 200;
(c) F.A. Cotton, L.M. Daniels, C.A. Murillo, P. Schooler, J. Chem. Soc., Dalton Trans. (2000) 2007;
(d) T. Ren, V. DeSilva, G. Zou, C. Lin, L.M. Daniels, C.F. Campana, J.C. Alvarez, Inorg. Chem. Commun. 2 (1999) 301;
(e) T. Ren, C. Lin, P. Amalberti, D. Macikenas, J.D. Protasiewicz, J.C. Baum, T.L. Gibson, Inorg. Chem. Commun. 1 (1998) 23;
(f) F.A. Cotton, L.M. Daniels, C.A. Murillo, P.J. Schooler, J. Chem. Soc., Dalton Trans. (2000) 2001;
(g) Y.-Y. Wu, J.-D. Chen, L.-S. Liou, J.-C. Wang, Inorg. Chim. Acta 36 (2002) 71;
(h) Y.-Y. Wu, Y.-C. Kao, J.-D. Chen, C.-H. Hung, Inorg. Chim. Acta 357 (2004) 1002.

[6] T. Ren, Coord. Chem. Rev. 175 (1998) 43.
[7] F.A. Cotton, K.J. Wiesinger, Inorg. Chem. 30 (1991) 871.
[8] T. Ren, S. Radak, Y. Ni, G. Xu, C. Lin, K.L. Shaffer, V. DeSilva, J. Chem. Crystallogr. 32 (2002) 197.
[9] G.M. Sheldrick, SHELXTL Release 5.03, Siemens Analytical X-ray Instruments Inc., Karlsruche, Germany, 1993.
[10] T. Ren, C. Lin, E.J. Valente, J.D. Zubkowski, Inorg. Chim. Acta 297 (2000) 283.
[11] K.M. Carlson-Day, J.L. Eglin, C. Lin, L.T. Smith, R.J. Staples, D.O. Wipf, Polyhedron 18 (1999) 817.
[12] J.L. Eglin, L.T. Smith, R.J. Staples, Inorg. Chim. Acta 351 (2003) 217.
[13] H.-Y. Weng, Y.-Y. Wu, C.-P. Wu, J.-D. Chen, Inorg. Chim. Acta 357 (2004) 1369.
[14] Y.-S. Yen, C.-W. Yeh, J.-D. Chen, J.-C. Wang, J. Cluster Sci. (2008), doi:10.1007/s10876-007-0154-5.
[15] F.A. Cotton, L.M. Daniels, I. Guimet, R.W. Henning, G.T. Jordan, C. Lin, C.A. Murillo, A.J. Schultz, J. Am. Chem. Soc. 120 (1998) 12531.
[16] F.A. Cotton, Z. Li, C.Y. Liu, C.A. Murillo, Q. Zhao, Inorg. Chem. 45 (2006) 6387.